New Incremental Actuators based on Electro-active Polymer: Conceptual, Control, and Driver Design Considerations.

Thummala, Prasanth; Schneider, Henrik; Zhang, Zhe; Andersen, Michael A. E.; Sarban, Rahimullah

Published in:
I E E E - A S M E Transactions on Mechatronics

Link to article, DOI:
10.1109/TMECH.2016.2533667

Publication date:
2016

Document Version
Peer reviewed version

New Incremental Actuators based on Electro-active Polymer: Conceptual, Control, and Driver Design Considerations

Prasanth Thummala[*], *Member*, *IEEE*, Henrik Schneider[$], *Member*, *IEEE*, Zhe Zhang[$], *Member*, *IEEE*, Michael A. E. Andersen[$], *Member*, *IEEE*, Sarban Rahimullah[#], *Member*, *IEEE*

***Abstract*—This paper presents an overview of the widely used conventional linear actuator technologies and existing electro-active polymer based linear and rotary actuators. It also provides the conceptual, control and driver design considerations for a new dielectric electro-active polymer (DEAP) based incremental actuator. The DEAP incremental actuator consists of three independent DEAP actuators with a unique cylindrical design that potentially simplifies mass production and scalability compared to existing DEAP actuators. To accomplish the incremental motion, a high voltage (HV) bidirectional DC-DC converter, independently charges and discharges each capacitive DEAP actuator. The topology used for the HV driver is a peak current controlled bidirectional flyback converter. The scalability of the proposed DEAP incremental actuator is discussed, and different scaled designs are provided. The estimated speeds and forces for various scaled incremental actuator designs are provided. The HV drivers are experimentally tested with a prototype of the DEAP incremental actuator. The energy efficiency measurement results of one of the HV driver are presented. The DEAP incremental actuator prototype achieved bidirectional motion with a maximum velocity of 1.5 mm/s, at 2.87 Hz incremental driving frequency, when all actuators are driven with 1.8 kV. Finally, two new improved concepts of DEAP based incremental actuator are presented.**

***Index Terms*—linear actuators, dielectric electro-active polymer (DEAP), scalability, DC-DC power converters, energy efficiency**

I. INTRODUCTION

ACTUATORS providing linear motion are used in a vast variety of applications ranging from large size machinery (e.g., cranes) to small scale micro-electro-mechanical system (MEMS) devices used for micro positioning. Linear actuators are typically characterized by their maximum stroke length, force, speed, and precision (or resolution). The typical linear actuators include an electro-mechanical, hydraulic, pneumatic, piezo, and electro-active polymer, etc.

An electromechanical linear actuator [1] uses a DC motor or a stepper motor to control a linear-action shaft output. Its advantages are high force, high speed, and high precision, and disadvantages are mechanical complexity, heavy weight and size, and high cost. A pneumatic linear actuator [2] operates with an external source of compressed air. It generates precise motion, but relatively complex to control via pressure valves and compressor manipulation. A hydraulic linear actuator [3] requires an external source for fluid pressurization. Hydraulic actuators not only allow the generation of large forces but also capable of closed-loop velocity controlling or highly precise positioning of heavy loads. Its control is complex, involving compressor and hydraulic valves. A piezo actuator [4] converts electrical energy directly into mechanical energy and vice versa. Besides a higher resolution, the piezo actuators have other advantages such as small size, light weight, operation under magnetic fields, low energy consumption, and low wear and tear. The disadvantages are high cost, low shock robustness, and requirement of high driving voltage [5].

The aforementioned standard linear actuators are mechanically complex systems. The stroke of these actuators is limited to their initial geometrical dimensions. This inherent characteristic limits their use in applications requiring large stroke and low size actuators. This motivates the research towards actuators based on novel smart materials. Incremental actuators are an alternative design to potentially overcome these limitations by providing an inchworm-like actuation. Dielectric electro-active polymer (DEAP) [6]-[12], due to its unique properties such as high flexibility (100,000 times less stiff than steel), large strain, high speed, and low weight (7 times lighter than steel) can potentially provide novel incremental actuator solutions. The DEAP incremental actuator technology can be used in various challenging industries such as, automotive, space and medical. Table I provides a comparison of DEAP technology with piezo and pneumatic actuator technologies, and electromechanical motors. To summarize, the DEAP incremental actuator technology has lower force density but has the potential for higher strain, better energy efficiency, and higher structural flexibility and robustness compared to other technologies. The

This work was supported by the Danish National Advanced Technology Foundation under the "Highly efficient low cost energy generation and actuation using disruptive DEAP technology" project, managed by Danfoss PolyPower A/S, Denmark.

Part of this paper was presented and selected as a best student paper award at the IEEE Energy Conversion Congress and Exposition (ECCE) USA'13 conference (Sept. 15-19th, 2013, Denver, CO, USA).

[*]The author is with the Electrical Machines and Drives Laboratory, Department of Electrical and Computer Engineering, National University of Singapore, 1 Engineering Drive 3, Singapore 117580 (email: prasanth.iitkgp@gmail.com).

[$]The authors are with the Department of Electrical Engineering, Technical University of Denmark, DK-2800 Kongens Lyngby, Denmark (email: hensc@elektro.dtu.dk, zz@elektro.dtu.dk, ma@elektro.dtu.dk).

[#]The author is with LEAP Technology, Science and Technology Park, DK-2800 Kongens Lyngby, Denmark (e-mail: Rahim@leaptechnology.com).

TABLE I
COMPARISON BETWEEN DEAP AND CONVENTIONAL ACTUATOR TECHNOLOGIES [13]

Parameter	DEAP Actuator Technology	Piezo Actuator Technology	Pneumatic Actuator Technology	Electromechanical Motors
Strain	Large (≈ 1-100%)	Small (≈ 0.02-0.1%)	Medium (≈ 1-60%)	Medium (≈ 5-40%)
Force density (Actuation stress)	Low (≈ 0.2-0.5 N/mm^2)	Medium (≈ 5-20 N/mm^2)	Low (≈ 0.5-0.9 N/mm^2)	High (≈ 50-200 N/mm^2)
Structural flexibility	High (Young's Modulus ≈ 1.1-2.8 MPa)	Low (Young's Modulus ≈ 40-60 GPa)	Medium (Young's Modulus ≈ 1-3 GPa)	Very low (Young's Modulus ≈ 150-250 GPa)
Incremental actuation frequency	Low (≈ 1-15 Hz)	High (≈ 100-5000 Hz)	Medium (≈ 50-100 Hz)	Very high (≈ 20-50 kHz)
Linear velocity per unit length = Strain×incremental actuation frequency	Medium (≈ 1-1500 Hz)	Low (≈ 20-500 Hz)	High (≈ 50-6000 Hz)	Very high (≈ 100-2000 kHz)
Efficiency	High (≈ 75-85%)	Medium (≈ 65-75%)	Low (≈ 30-40%)	Medium (≈ 50-70%)
Mass density	Low (≈ 900-1200 kg/m^3)	Medium (≈ 2500-5000 kg/m^3)	Very low (≈ 180-250 kg/m^3)	High (≈ 7000-10000 kg/m^3)

DEAP technology is an emerging technology and future performance improvements are expected.

Several researchers have investigated and implemented EAP based linear and rotary type actuators. Numerous applications of dielectric elastomers including an inchworm robot and rotary motors have been described in [14]. A robotic inchworm in [14] uses electrostatic clamps which enable it to travel over both vertical and horizontal surfaces, for tasks such as inspection in narrow pipes, etc. A rotary motor made with a pair of bow tie elastomer actuators, with an output power of 4 W at 100 RPM has been demonstrated in [14]. A segmented DE-driven inchworm concept has been described in [15]. Each segment consists of a single tube, two DE membranes, and a coupling fluid. The walking robot using a multi-functional electro elastomer (MER) spring roll as each of the robot's six legs is provided in [16]. Each spring roll leg was a linear actuator, with 3-6 mm stroke at 1-10 Hz frequency. The emerging DE technology has been thoroughly reviewed and presented exciting possibilities across a wide range of applications including soft robotics [17]. An earthworm robot has been made using a novel soft actuator based on a dielectric elastomer. It has been demonstrated that the actuator moved with 1 mm/s at 5 Hz [18]. A simple rotary motor based on dielectric elastomers has been proposed in [19]. A new way to achieve the rotary motion using the DEAP actuators has been reported in [20].

The proposed incremental actuator concepts based on DEAP are aimed to produce a linear motion. Two types of incremental motion namely pusher and walker are identified for the DEAP based incremental actuators. In pusher mode, the actuator is stationary and pushes an external system incrementally while in walker mode the actuator itself moves on a stationary surface or cavity. The generic concept of an incremental actuator is an assembly of sub-mechanism capable of gripping, releasing and extending. The concept 1 DEAP incremental actuator proposed in [21], consists of two grippers at both ends (to enable gripping operation) and an extender (to move the grippers) as shown in Fig. 1. Each gripper and an extender are made using an axial DEAP actuator. Simple design, low noise operation, high energy efficiency, and low cost are the key advantages of the DEAP based incremental actuators compared to the conventional linear incremental actuators or other sliding dielectric elastomer actuators.

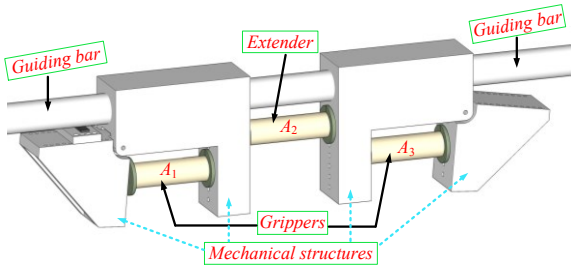

Fig. 1. Concept 1 of the DEAP incremental actuator [21], [41].

Driving a DEAP incremental actuator has three main challenges from a power electronics perspective. Firstly, it requires high voltages (2-2.5 kV), to generate sufficient force and stroke from each axial DEAP actuator. Suitable energy sources for this application are lithium batteries with a voltage range of 9-24 V DC. This necessitates the need of high voltage step-up circuits as a driving mechanism for the DEAP incremental actuator. Secondly, DEAP actuators convert only a small fraction of the input electrical energy into mechanical work, while they store the remainder in the capacitive structure of the actuator, and must be recovered to maximize the system efficiency. This necessitates the need of bidirectional converters [22]-[24]. Finally, to move the DEAP incremental actuator with a given speed and direction, the three DEAP actuators need to be driven by a specific sequence of HV signals.

The magnetic transformer based flyback converter is suitable for high voltage and low power applications due to its simple structure and low component count [25]. High voltage switch-mode power supplies for charging the capacitive loads have been implemented in [26], [27]. The bidirectional flyback converters are proposed in [28]-[30] to transfer the power in both directions. However, those topologies cannot be directly used for charging and discharging a capacitive load at high voltage (2.5 kV). Prior work on the high voltage drivers for the DEAP actuators demonstrated a low voltage piezoelectric transformer based DEAP solution, and it was incorporated into a coreless DEAP actuator [31], and a modified bidirectional

flyback converter topology to drive the PolyPower Push Inlastor DEAP actuator [32], [33]. The flyback transformer is the most critical component in the HV flyback converter. Selecting the best transformer winding architecture (TWA) and optimizing the HV transformer using it, would lead to an improved energy efficiency of the HV converter. In [34] an efficiency optimization technique is proposed for a bidirectional flyback converter. Several high voltage transformer winding architectures (TWAs) have been investigated in [35]. Control algorithms for optimal-flyback charging of a capacitive load have been proposed in [36], which focuses mainly on minimizing the conduction losses in the converter. Digital control of the bidirectional flyback converter is proposed in [37], for improving energy efficiency and the charge and discharge speed (driving frequency) of the incremental motor. Intelligent control of EAP actuators based on fuzzy and neuro-fuzzy methodologies is proposed in [38]. An experimental study of DEAP actuator energy conversion efficiency is performed in [39]. Geometry optimization of tubular dielectric elastomer actuators with anisotropic metallic electrodes is discussed in [40]. The detailed actuator design, HV power electronics, and practical implementation for inchworm actuators is not properly discussed in the literature.

The objectives of this paper are: to provide the conceptual design and scalability of the axial DEAP actuators used in the DEAP based incremental motor and to test the proposed DEAP incremental actuators with the necessary control and HV driving circuits. The paper is organized as follows: following the introduction, Section II discusses the conceptual design of an axial DEAP actuator, followed by the scalability of DEAP actuators in Section III. Section IV describes the basic idea and operational diagrams of the proposed DEAP incremental actuator concept. Section V presents high voltage driving circuits for the DEAP incremental actuator, the experimental results, and the system integration results. Section VI describes the two improved DEAP incremental actuator concepts. Finally, Section VII concludes the paper.

II. Conceptual Design of an Axial DEAP Actuator

An axial DEAP actuator is a tubular structure being formed by rolling a DEAP sheet as shown in Figs. 2(a) and 2(b). The main design parameters of such structure are its active height H_a, passive height H_p, inner diameter D_i, outer diameter D_o, and the number of laminate layers n_l. The dielectric elastomer (DE) film consists of two DE sheets laminated together. Core DE technology comprises an electrical insulating layer of elastomer sandwiched between two deformable layers of electrically conductive material (electrodes). As shown in Fig. 2(c), only one of the DE sheets of a DE laminate is metallized at either lateral end to the left and to the right. This is to realize a safe electrical connection in the actuator by avoiding short circuiting. Some of the design parameters are assumed before the design and the remaining parameters are calculated using the known parameters. The mechanical and electrical constants of the actuator are provided in Table II.

The capacitance of the DEAP actuator at no applied voltage is given by

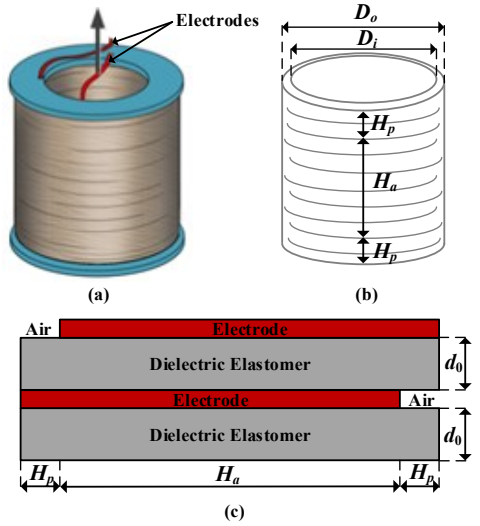

Fig. 2. Conceptual drawing of an axial DEAP actuator: (a) Finished actuator with end mounts and connecting wires, (b) Dimensional drawing of the DEAP cylindrical design, (c) Schematic of a laminated film cross-section with active and passive ends.

TABLE II
Mechanical and Electrical Constants and Design Parameters of the DEAP Actuator

Parameter	Value
Permittivity of vacuum ε_0	8.854×10^{-12} F/m
Relative permittivity of the dielectric material ε_r	2.9
Young's modulus of the transducer Y_t	2.7 MPa
The sum of Mooney constants for the transducer $C_1+C_2 = Y_t/8$	0.34 MPa
Initial thickness of the polymer film d_0	45 μm
Active height of the transducer H_a	70 mm
Height of each passive end H_p	20 mm
Total width of the rolled DEAP sheet W	10 m
Maximum operating electric field strength E_{max}	45 V/μm
Maximum operating voltage $V_{applied,max}$	2025 V
Inner diameter of the DEAP actuator D_i	25 mm

$$C_{DEAP} = \varepsilon_0 \varepsilon_r \frac{WH_a}{d_0} = 400 \text{ nF} \quad (1)$$

where ε_0 and ε_r are the electrical permittivities of vacuum and dielectric material respectively, W is the total width of the rolled DEAP sheet, and d_0 is the thickness of the polymer film at no applied voltage.

The number of laminate layers n_l is calculated using the following expression

$$n_l = \frac{D_o - D_i}{2d_0} = \frac{\sqrt{\left(\frac{4}{\pi} W d_0 + D_i^2\right)} - D_i}{2d_0} = 107 \quad (2)$$

The outer diameter of the rolled DEAP actuator is given by

$$D_o = D_i + 2n_l d_0 = 35 \text{ mm} \quad (3)$$

The cross-sectional area of the active material is given by

$$A_c = Wd_0 = 450 \text{ mm}^2 \tag{4}$$

The total volume of the polymer material is given by

$$V_c = Wd_0\left(H_a + 2H_p\right) = 49.5 \text{ cm}^3 \tag{5}$$

The equation governing the electrostatic $F_{Electrostatic}$, elastic $F_{Elastic}$ and load forces F_{load} in a DEAP actuator system as shown in Fig. 3 during static operation is given by

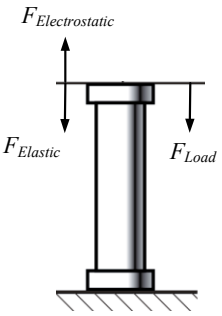

Fig. 3. Force balance of DEAP actuator element in static operation.

$$F_{Electrostatic} - F_{Elastic} = F_{load} \tag{6}$$

Equation (6) can be simplified as [6], [42] and [43]

$$\left[\varepsilon_0\varepsilon_r\left(\frac{V_{DEAP}}{d_0}\right)^2\alpha^2 A_c\right] - \left[2(C_1+C_2)\left(\alpha^2-\alpha^{-2}\right)A_c\right] = F_{load} \tag{7}$$

where V_{DEAP} is the applied voltage to the DEAP actuator, α represents the stretch (elongation) ratio and is defined as, α=1+s, where s is the strain in the compliant direction, and C_1+C_2 is the sum of Mooney constants for the transducer with $C_1 + C_2 = \frac{Y_t}{8}$ and Y_t is the Young's modulus of the transducer. The stroke of DEAP actuator is sH_a. The influence of passive ends has been ignored, as the displacement between passive ends and active area is much smaller than the stroke of the transducer.

The output force of the DEAP actuator is given by

$$F_{output} = \left[\varepsilon_0\varepsilon_r\left(\frac{V_{DEAP}}{d_0}\right)^2\alpha^2 A_c - \frac{Y_t}{4}\left(\alpha^2-\alpha^{-2}\right)A_c - F_{load}\right] \tag{8}$$

Since the displacement between the active and passive areas is limited, so we could assume that they are linear material, and the passive area has the same modulus of elasticity as that of the active area. In the equilibrium position, the stress on the passive area should be equal to the stress of the active area, therefore

$$Y_t\frac{\Delta L}{H_p} = \varepsilon_0\varepsilon_r\left(\frac{V_{DEAP}}{d_0}\right)^2 - Y_t\frac{2\Delta L}{H_a} \tag{9}$$

where ΔL is the displacement between the active and passive ends.

The displacement ΔL is given by

$$\Delta L = \frac{\varepsilon_0\varepsilon_r\left(\frac{V_{DEAP}}{d_0}\right)^2}{Y_t\left(\frac{1}{H_p}+\frac{2}{H_a}\right)} \tag{10}$$

Blocking force can be reduced by the passive ends of the transducer, due to the displacement between the passive and active areas. The blocking force is given by the following expression,

$$F_{blocking} = \left(\varepsilon_0\varepsilon_r\left(\frac{V_{DEAP}}{d_0}\right)^2 - Y_t\frac{2\Delta L}{H_a}\right)\cdot Wh_0 = Y_t\frac{\Delta L}{H_p}\cdot Wh_0 \tag{11}$$

The operating region of an axial DEAP actuator can be represented by the relationship between its force, stroke and applied voltage (or electric field strength). The force-stroke, stroke-voltage and force-electric field strength characteristics of the axial DEAP actuator which is designed above, are shown in Figs. 4, 5 and 6, respectively. As shown in Fig. 4, to achieve a certain stroke, the output force of the actuator decreases with the applied voltage. Also, for a given applied voltage, the output force drops as the actuator elongates. The variation of the stroke and strain of the DEAP actuator as a function of the applied voltage are provided in Fig. 5. The

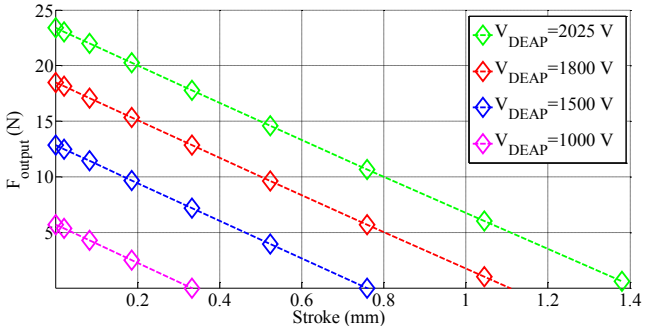

Fig. 4. Modeled actuator output force as a function of stroke for the different maximum applied voltages (for F_{load}=0 N).

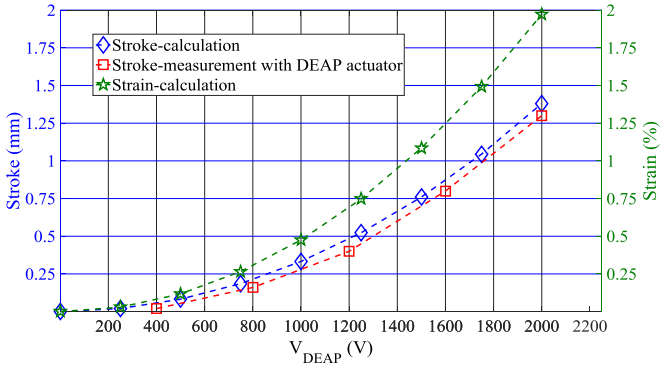

Fig. 5. Modeled actuator stroke and strain, and measured actuator stroke as a function of applied voltage.

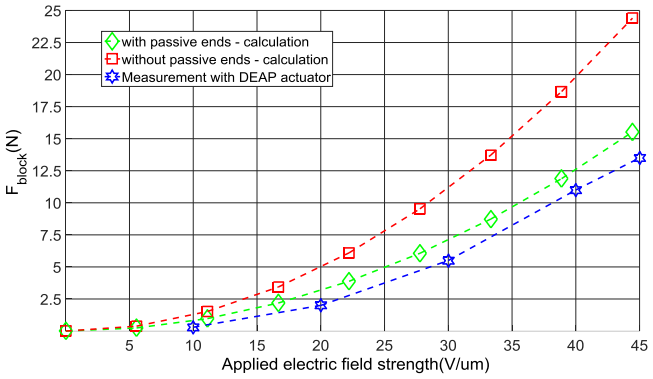

Fig. 6. Modeled and measured blocking force as a function of applied electric field strength.

measured stroke of the DEAP actuator is also provided in Fig. 5. The calculated blocking force of the actuator with and without passive ends and the measured blocking force are provided in Fig. 6. From Fig. 6, it is clear that the blocking force is less for the actuator which has passive ends, compared to the actuator without passive ends.

III. Scalability of DEAP Actuators

One of the unique features of DEAP actuator elements is their ease of scaling. DEAP actuator elements can be scaled up to provide larger actuation forces by increasing the cross section areas as shown in Figs. 7 and 8, i.e. rolling more DEAP material. Similarly, DEAP actuator elements can be scaled up easily to provide larger actuation stroke by increasing the length of the DEAP actuator element. The upscaling can also be achieved by connecting multiple actuator elements in series or parallel resulting in larger stroke or force, respectively.

To investigate the scalability of the DEAP incremental actuator, three designs as shown in Table III are considered. The reference actuator design parameters are provided in Table II. In the scaled design 1, the actuator's height is reduced by 10 times, by keeping the area of cross-section same as that of the reference design. In the scaled design 2, the area of the cross-section of the actuator is reduced by 10 times, by keeping its length the same as the reference. The scaled design 3 is made by reducing both the actuator's length and its area of cross-section by 10 times. The characteristics of scaled designs 1 and 2 are shown in Figs. 9(a), 9(b), and 9(c), 9(d), respectively. Similarly, the characteristics of scaled design 3 are provided in Fig. 9(e). For the scaled design 1, since the actuator's length is reduced by 10 times, the stroke as shown in Fig. 9(a) is very low, even at 2 kV. Since the area of cross-section is not changed the output force is not reduced as shown in Fig. 9(b). For the scaled design 2, since the area of cross-section is reduced by 10 times, the output force is reduced as shown in Fig. 9(c), but the stroke remains the same as the reference design. The blocking force is also reduced for the scaled design 2, as shown in Fig. 9(d). Similarly, for the scaled design 3, the force-stroke characteristics are shown in Fig. 9(e), in which the stroke and force both are reduced. In Fig. 9(e), the actuator when driven with 1.8 kV can only produce 1 N output force for a stroke of 0.05 mm.

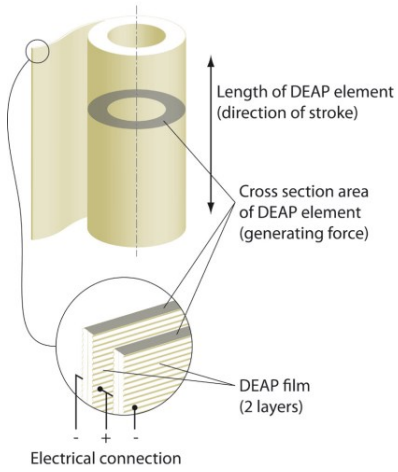

Fig. 7. Rolled structure construction, where the electrode elasticity allows axial actuation.

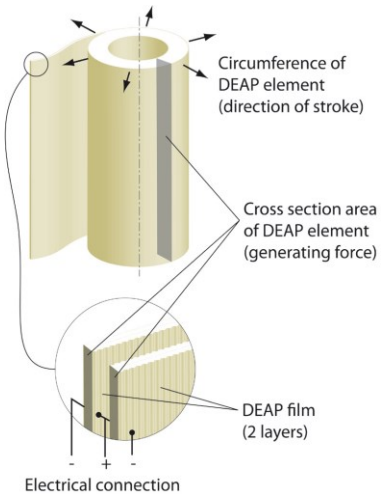

Fig. 8. Rolled structure construction, where the electrode elasticity allows radial actuation.

TABLE III
Design Parameters of the Scaled DEAP Actuator

Parameter	Scaled design 1	Scaled design 2	Scaled design 3
Active height of the transducer H_a	7 mm	70 mm	7 mm
Height of each passive end H_p	2 mm	20 mm	2 mm
Total width of the rolled DEAP sheet W	10 m	1 m	1 m
Center hole diameter of the actuator D_i	25 mm	4 mm	4 mm
The outer diameter of the actuator D_o	35 mm	9 mm	9 mm
Capacitance of the scaled actuator C_{DEAP}	40 nF	40 nF	4 nF
Number of layers of laminate n_l	107	51	51
Area of cross section of active DEAP A_c	450 mm^2	45 mm^2	45 mm^2

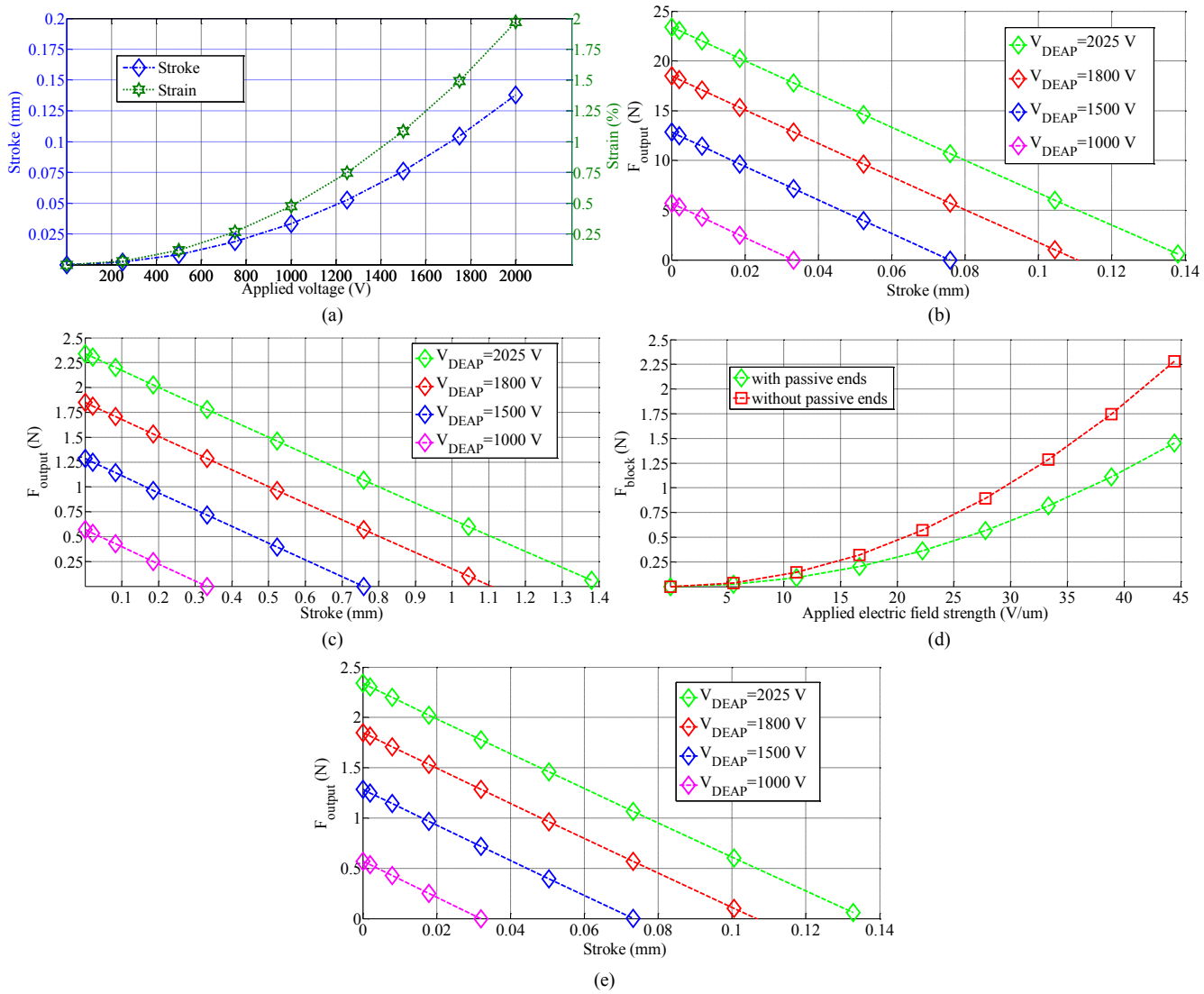

Fig. 9. a) Actuator stroke and strain as a function of applied voltage for the scaled design 1; b) Actuator output force as a function of stroke for different maximum applied voltages for the scaled design 1; c) Actuator output force as a function of stroke for different maximum applied voltages for the scaled design 2; d) Blocking force as a function of applied electric field strength for the scaled design 2; e) Actuator output force as a function of stroke for different maximum applied voltages for the scaled design 3.

IV. Control of Incremental Motor

The control (or driving) sequence for concept 1 of the incremental actuator is provided in this section. The concept 1 consists of three axial DEAP actuators (one extender and two grippers). The incremental actuation sequence and the driving voltage waveforms for the grippers and the extender are shown in Figs. 10 and 11, respectively [21]. Each gripper is connected to mechanical supports on either side. It expands and clamps to the guiding bar (e.g., a rod) surface when charged (with high voltage), and unfastens from it when discharged. The extender expands axially along the guiding bar. During the operation, one gripper holds the guiding bar while the other gripper is in a released position. The extender either pushes or pulls the released gripper. The incremental actuator performs six different steps, to achieve a single incremental actuation stroke Δx as shown in Fig. 10. In Fig. 11, V_{ch1}, V_{ch2},…, V_{ch6} are the enable signals for the gate drivers of the three HV DC-DC converters, respectively, and V_{A1}, V_{A2}, and V_{A3} are the voltages across the DEAP actuators A_1, A_2, and A_3, respectively.

A. Moving sequence for the linear incremental motion towards the positive x-axis direction

1. *Start*: All actuators are in the discharged state.
2. *Step* 0 (S_0): A_1 is charged and clamps to the guiding bar. A_2 and A_3 are in the discharged state.
3. *Step* 1 (S_1): A_1 remains in the charged state. A_2 is charged and pushes the mechanical structure towards right, and A_3 remains in the discharged state.
4. *Step* 2 (S_2): A_1 and A_2 still remain in the charged state. A_3 is charged.
5. *Step* 3 (S_3): A_1 is discharged and is in the release position. A_2 and A_3 still remain in the charged state.

6. *Step* 4 (S_4): A_1 remains in the discharged state. A_2 is discharged, and A_3 remains in the charged state.
7. *Step* 5 (S_5): A_1 is charged. A_2 remains in the discharged state, and A_3 remains in the charged state.
8. *Step* 6 (S_6): A_1 remains in the charged state. A_2 remains in the discharged state, and A_3 is discharged.
9. *End*: All actuators are discharged at the end.

The Step 0 is only used for charging the actuator A_1. The Steps 1-6 (S_1-S_6) repeat for achieving continuous incremental actuation cycles. The End step is used to discharge all actuators.

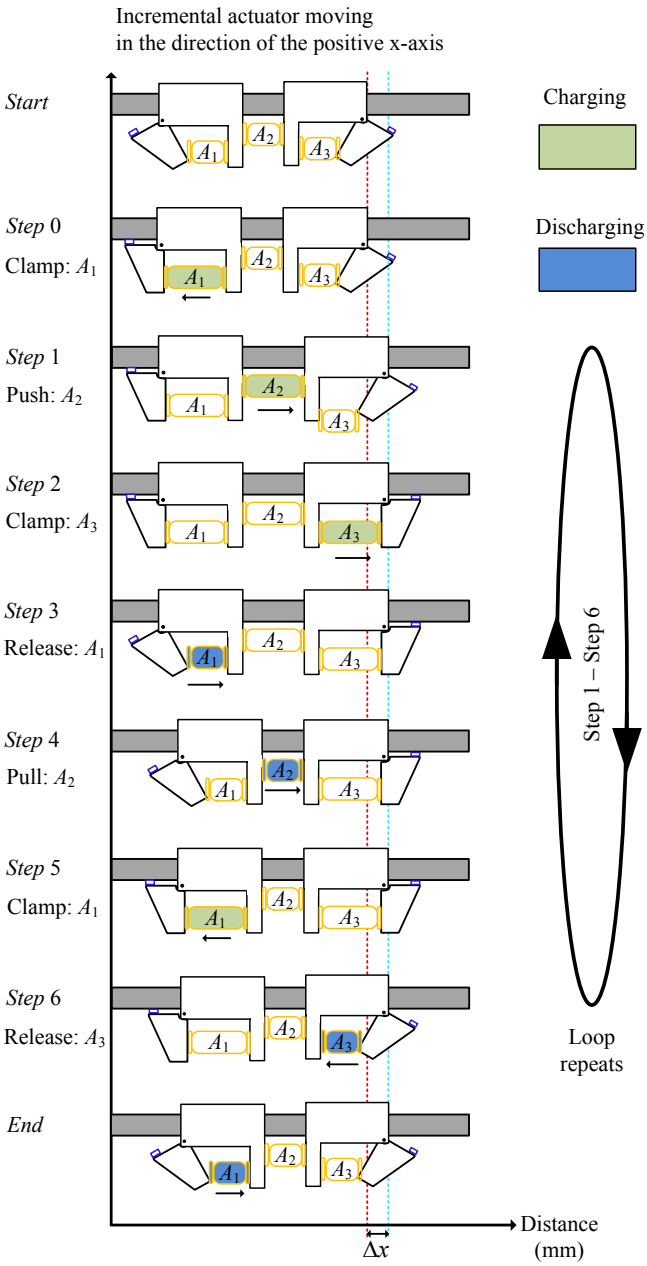

Fig. 10. Moving sequence of the DEAP incremental actuator for incremental motion towards the positive x-axis direction.

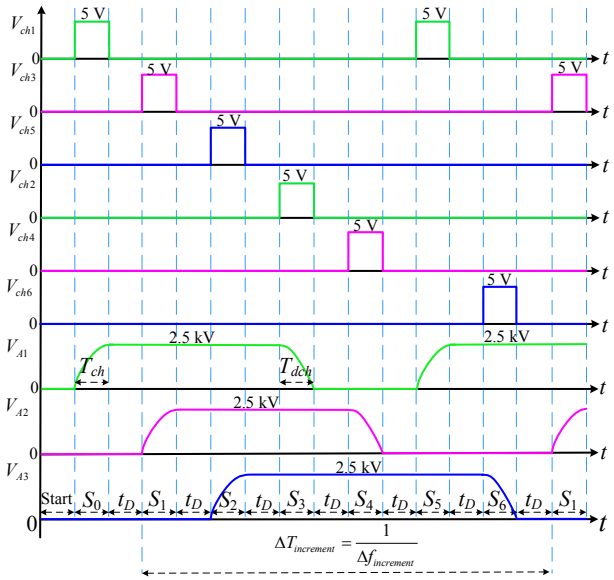

Fig. 11. Enable signals and driving voltages of all DEAP actuators, to achieve the incremental motion with variable speed, towards the positive x-axis direction.

B. *Incremental driving frequency*

Assuming the same charging T_{ch} and discharging T_{dch} times for all DEAP actuators, the maximum incremental driving frequency $\Delta f_{increment\_max}$ or minimum incremental period $\Delta T_{increment\_min}$ is given by

$$\Delta f_{increment\_max} = \frac{1}{6\left(T_{ch} + T_{dch}\right)} = \frac{1}{\Delta T_{increment\_min}} \tag{12}$$

The incremental actuator speed can be changed, by providing a delay t_D between the charge and discharge cycles of actuators A_1, A_2, and A_3. The expression for the incremental driving frequency $\Delta f_{increment}$ or incremental period $\Delta T_{increment}$ is given by

$$\Delta f_{increment} = \frac{1}{6\left(T_{ch} + T_{dch}\right) + 6t_D} = \frac{1}{\Delta T_{increment}} \tag{13}$$

When the DEAP incremental actuator is loaded during the operation, the delay between the steps S_1 and S_2 can be skipped. This can prevent pulling of the incremental actuator by the load when actuator A_2 is charged.

C. *Velocity estimation for the scaled actuator designs*

It is very interesting to estimate the velocity of the DEAP incremental actuator for all scaled axial DEAP actuators. Figure 12 provides the estimated velocity as a function of the incremental drive frequency (see Eq. (13)) for all designs discussed in Sections II and III. The viscous effects of the polymer material have been neglected. The speed of the incremental motor for the reference and each scaled design is estimated when all actuators are driven with 1.8 kV. Inorder to make a fair comparison among all scaled actuator designs, the speed for each scaled actuator is estimated for the same output force of 1 N, and compared with the reference design with 1 N and 10 N output forces.

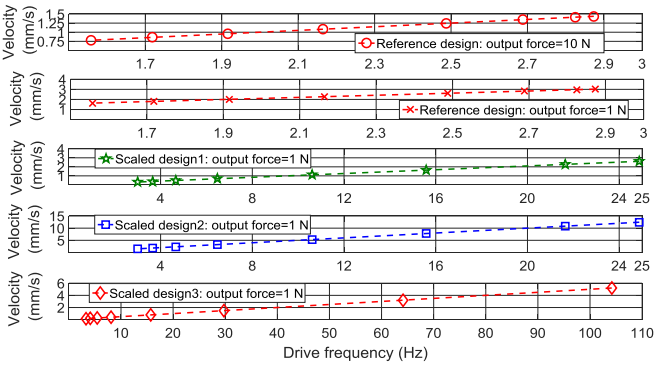

Fig. 12. Estimated velocity of the DEAP incremental actuator for different designs, for a driving voltage of 1.8 kV.

For the reference design, to produce an output force of 1 N and 10 N, the velocity of the actuator varies between 1.6-3 mm/s, and 0.8-1.4 mm/s, respectively, as shown in Fig. 12. For the scaled design 1, the velocity changes between 0.31-2.61 mm/s. Similarly, for the scaled design 2, the velocity varies between 1.5-12.4 mm/s. Finally, for the scaled design 3, the velocity changes between 0.16-5.2 mm/s. Compared to the reference design (with 1 N output force), the scaled designs 1, 2 and 3 produce relatively the same maximum speed, very high maximum speed and slightly high maximum speed, respectively. The drive frequency for all scaled designs is not the same, since the scaled DEAP actuators' capacitances are different. The simulated charge and discharge times for the reference and scaled designs with capacitances 400 nF, 40 nF, and 4 nF are 21 ms, 2.1 ms, and 240 μs, and 36 ms, 3.6 ms, and 360 μs, respectively. The delay times (t_D) used for the calculation of the driving frequency for each design are 1 ms, 2 ms, 5 ms, 10 ms, 20 ms, 30 ms, 40 ms, and 50 ms, respectively.

The performance specifications of the several designed incremental motors (at an applied voltage of 1.8 kV) are summarized in Table IV. The reference design (with 1 N output force) has the highest volume and maximum resolution. The scaled design 3 has the lowest volume and minimum resolution. The scaled designs 1 and 2 have same volume. Nevertheless, scaled design 2 has higher resolution compared to scaled design 1. The scaled design 2 produces maximum velocity among all designs. The resolution is the stroke of an extender in a single incremental step. The measured velocity of incremental motor can be found in Section V (Table VI).

TABLE IV
PERFORMANCE SPECIFICATIONS OF THE DESIGNED DEAP INCREMENTAL ACTUATORS

Incremental motor performance specifications	**Reference design**		**Scaled design 1**	**Scaled design 2**	**Scaled design 3**
Velocity	0.8-1.4 mm/s	1.6-3 mm/s	0.31-2.61 mm/s	1.5-12.4 mm/s	0.16-5.2 mm/s
Push/Pull force	10 N	1 N	1 N	1 N	1 N
Holding force	10 N	1 N	1 N	1 N	1 N
Resolution	0.5 mm	1.05 mm	0.1 mm	0.5 mm	0.05 mm
Total volume	49.5 cm^3		4.95 cm^3	4.95 cm^3	0.495 cm^3

V. POWER ELECTRONICS

A. HV drivers

The complete circuit diagram of the DEAP incremental actuator driven by three bidirectional high voltage DC-DC converters is provided in [21]. The topology is a peak current controlled bidirectional flyback converter. Three bidirectional flyback converters are powered by the same source. Each converter independently controls the charge and discharge operations of the three axial DEAP actuators (two grippers and an extender) in the DEAP incremental actuator.

Three high voltage bidirectional flyback converters are experimentally tested with both film capacitor loads and the DEAP incremental actuator. The picture of the experimental prototype with film capacitor loads is shown in Fig. 13. The setup of the DEAP incremental actuator with the axial DEAP actuators is shown in Fig. 14. The converter design specifications are provided in Table V.

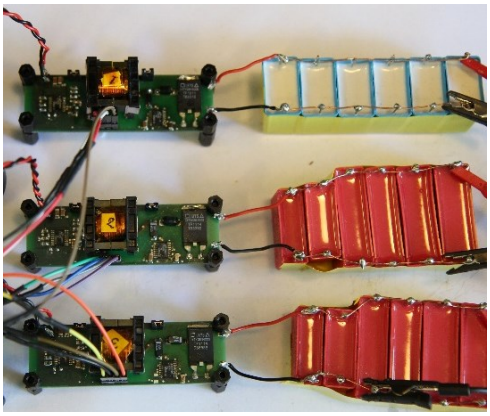

Fig. 13. Experimental setup with the three HV bidirectional flyback converters driving film capacitive loads.

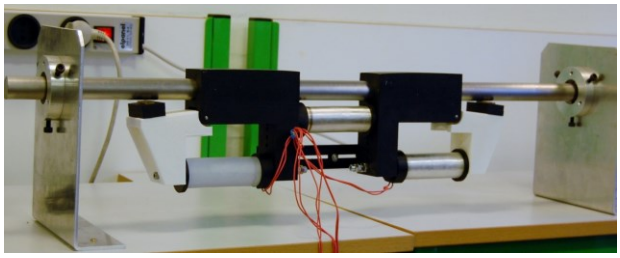

Fig. 14. Setup of the DEAP incremental actuator driven by three HV drivers.

TABLE V
CONVERTER DESIGN SPECIFICATIONS

Parameter	**Value**
Input voltage	24 V
Output voltage	0-2500 V
Capacitance of each DEAP actuator in the DEAP incremental actuator setup	400 nF
Capacitance of each film capacitor load	200 nF
Incremental driving frequency	~ 1-5 Hz
Primary peak current during charging / discharging process	4.2 A / 5.3 A

The capacitance of each film capacitor load shown in Fig. 13 is 200 nF. The capacitance of each axial DEAP actuator in the setup shown in Fig. 14 is 400 nF. The detailed design of the bidirectional flyback converter for driving a capacitive load is discussed in [44]. During charge process the converter operates in boundary conduction mode (BCM), and during discharge process it operates in discontinuous conduction mode (DCM) using a control IC LT3751 [45]. Practical experience reveals that careful design of the flyback transformer with low leakage inductance and low self-capacitance is required for achieving high energy efficiency at high voltage bidirectional operation. The HV MOSFET used for this research was IXTV03N400S (4 kV, 300 mA, 290 Ω) [46]. Currently, the available high voltage MOSFET for this application is IXTA02N450HV (4.5 kV, 200 mA, 750 Ω) [47]. The HV diode used in the converter was SXF6525 (5 kV, 150 mA). Improper HV flyback transformer design may lead to failure of the HV MOSFET during the discharging operation.

B. *Energy efficiency of HV drivers*

The HV drivers as shown in Fig. 13 are not optimized in terms of efficiency. The measured charge and discharge energy efficiencies [32] of one of the HV driver with film capacitor loads (200 nF) are provided in Fig. 15. The maximum energy efficiency of the converter during charging operation (transferring the input energy to the actuator) is 87%, and during discharging operation (transferring the actuator energy back to the source) is 79%. The discharge energy efficiency is less than the charge energy efficiency, due to very high conduction losses, switching loss due to leakage inductance and capacitive switching losses of the HV MOSFET. Further research has been conducted to improve the energy efficiencies of HV drivers. The energy efficiency of an optimized HV driver is provided in Fig. 16. The charge and discharge energy efficiencies of the optimized converter to charge the film capacitive load (400 nF) from 0 V to 2.5 kV and vice versa are 89% and 84%, respectively.

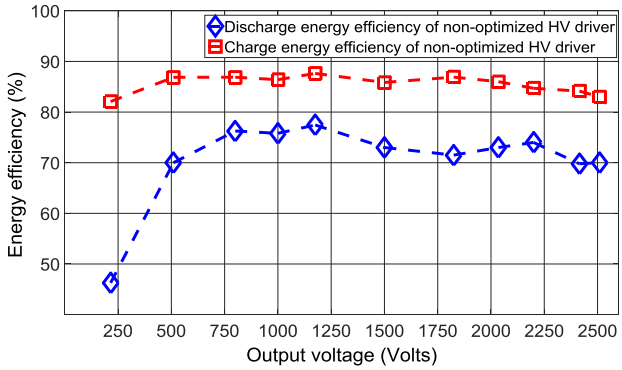

Fig. 15. Energy efficiency of the non-optimized HV driver with a 4 kV MOSFET on secondary HV side.

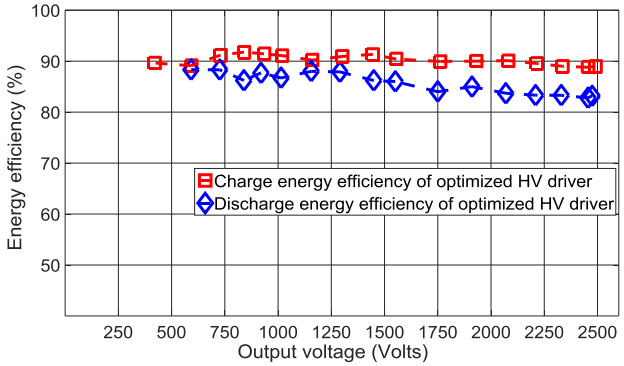

Fig. 16. Energy efficiency of the optimized HV driver with a 4 kV MOSFET on secondary HV side [37].

C. *System integration*

The integrated system of concept 1 incremental actuator as shown in Fig. 14 has been tested for its variable speed and repeatability. 100 increments are generated using the digital controller, and the total displacement and travel time are recorded. The maximum applied voltage is fixed to 1.8 kV to avoid any potential damage to the transducers. Table VI provides the acquired data of the experiments. It can be seen from Table VI that the system has a repeatability within 5% (of stroke) for different speeds. The DEAP incremental actuator achieved a maximum speed of 1.5 mm/s for a travel distance of 39 mm.

TABLE VI
EXPERIMENTAL DATA OF DEAP INCREMENTAL ACTUATOR MOVING WITH DIFFERENT SPEEDS TO ACHIEVE 100 INCREMENTS/STEPS

Total travel* (mm)	Total travel time (s)	Delay time t_D (ms)	Average Speed (mm/s)	Increment size / stroke per step (mm)	Incremental driving frequency $\Delta f_{increment}$ (Hz)
39	50	50	0.78	0.39	1.55
39	45	40	0.86	0.39	1.72
39	40	30	0.97	0.39	1.91
38	35	20	1.07	0.38	2.16
40	30	10	1.33	0.40	2.49
40	28	5	1.43	0.40	2.68
39	25	2	1.56	0.39	2.82
39	26	1	1.50	0.39	2.87

*All 3 DEAP actuators are driven with a maximum voltage of 1.8 kV. Practical charging time T_{ch}=23 ms, discharging time T_{dch}=36 ms.

D. *Discussion*

The DEAP incremental actuator technology has the potential to be used in various challenging applications. For using the DEAP actuators in such applications, the HV drivers should have a low volume to fit inside or above the actuators. The overall energy efficiency of battery-powered HV driver influences, the distance traveled by the incremental actuator. Hence, for DEAP actuator applications, both volume and energy efficiency of high-voltage drivers are extremely important and need to be optimized. From Fig. 16, it is clear that to charge the DEAP actuator from 0 V to 2.5 kV, only 11% input energy has been lost. And to discharge the DEAP actuator from 2.5 kV to 0 V, 16% remaining energy in the actuator has been lost. Therefore, an overall 25.2% input energy has been lost in a single charge and discharge switching cycle. When the driving voltage is lower than 2.5 kV, the energy loss will be much lower. This is a clear indication that DEAP can compete with the conventional actuator technologies in terms of energy efficiency. With a DEAP actuator, it is possible to hold/grip the position without loss of energy. Nevertheless, stepper motors would require

constant current to do the same. The series resistance of DEAP actuators is very low (~ 5-10 Ω), which is of the same order of flyback transformer secondary HV side resistance. The parallel resistance of DEAP actuators is very high (~ 10-20 GΩ), due to which the output voltage discharge during the charge or delay process is very slow. Using the proposed charge and discharge control schemes, the charge or energy has not been dumped by the actuator, instead it was recycled in every incremental cycle. Transferring an electrical energy between two dielectric elastomer actuators has been discussed in [48]. For the proposed DEAP incremental actuator, only a single axial DEAP actuator is either charged or discharged in any one of the six incremental actuation steps. Hence, the energy stored in all three actuators in the DEAP incremental motor is transferred to the single energy source, which makes the DEAP based incremental motor system more efficient.

VI. Improved Concepts of DEAP Incremental Actuators

The concept 1 incremental motor is bulky. Therefore, two new concepts (2 and 3) of DEAP incremental actuator with better compactness are provided in this section. Each concept has its unique characteristics which can demonstrate various unique properties of DEAP.

A. Concept 2

Concept 2 is proposed for operating outside or inside a cylindrical bar. Figure 17(a) demonstrates the concept 2 of the incremental actuator for crawling on the top of a cylindrical bar. It consists of three sub-components, namely one extender and two grippers at either end. The corrugation profiles of the extender and the grippers are 90° shifted. When in operation, one gripper holds the bar while the other gripper is in the released position. The extender either pushes or pulls the released gripper. The grippers are rolled on a core with radial tension. Rigid mechanical connections are subsequently applied. The extender sub-component can be realized by simply using a cylindrical actuator. The grippers and the extender are joined by gluing or screwing their mechanical connections together (green plates in Fig. 17(a)). Mechanical constrainers can be applied to the grippers in order to avoid the axial extension of the grippers when in operation. Such constrainers enable the gripper to exhibit only radial movements. Soft encapsulation for protection and/or aesthetics can be applied as shown in Fig. 17(b).

Figure 17(c) shows the concept 2 of the incremental actuator for crawling inside a cylindrical tube. It also consists of one extender and two grippers on either end. Both the grippers and the extender are cylindrical actuators. Additional gripping mechanisms are applied to the grippers (red structures in Fig. 17(c)). The gripping mechanism extends or contracts radially when the grippers are contracted or extended axially, respectively, as illustrated by the arrows in Fig. 17(c). The extender either pushes or pulls the contracted gripper. The arrows in the middle actuator indicate the expansion force. All three actuators provide an axial expansion force while the grippers translate the axial expansion force to a radial grip/release. The middle actuator uses the axial expansion force to axial elongation i.e. the stroke of the incremental

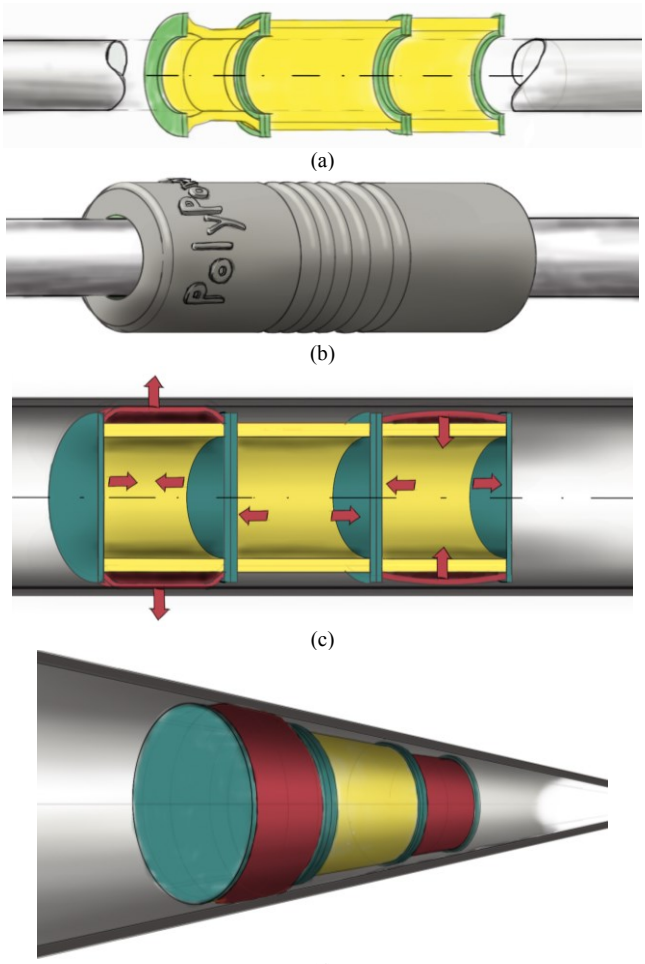

Fig. 17. Concept 2 of DEAP incremental actuator. (a) Cross section view of the actuator for crawling on the top of a cylindrical bar; (b) Incremental actuator with protective and/or aesthetic encapsulation; (c) Cross section view of the actuator with operational arrows for crawling in a cylindrical bar; (d) Full view of the incremental actuator [40].

actuator system. The three cylindrical actuators are joined together at their mechanical connections, by gluing or screws. Figure 17(d) illustrates a full view of the incremental actuator for moving inside a tube.

B. Concept 3

The concept 3 as shown in Fig. 18(a) is based on 3 DEAPs in an axial configuration. It consists of 1 extender and 2 blocking DEAPs. When the blocking DEAP is extended the wedges are driven towards the guide rod, thereby creates a blocking force. Here, three cylindrical transducers are used to facilitate the incremental motion. The outer two actuators are equipped with auxiliary mechanics such that the axial elongation of those transducers is transformed into a radial gripping on the pipe, hence these two actuators are conceptually designed to perform the gripping operation. The middle transducer is intended to be the extender/translator actuator. Auxiliary mechanics as shown in Figs. 18(b) and 18(c) are attached to the transducer enabling them to grip, release and extend on a solid rod.

The concept 3 mechanical system has been fabricated in Danfoss PolyPower. The transducers were mounted with the

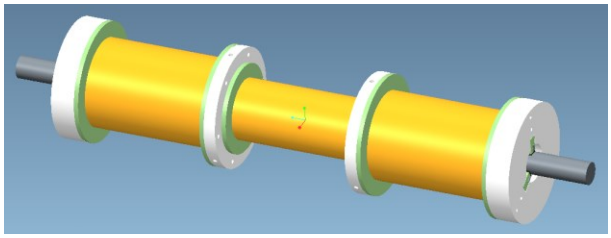

(a)

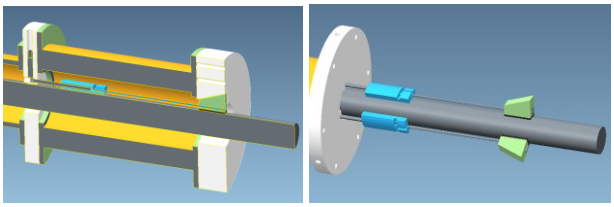

(b) (c)

Fig. 18. (a) Concept 3 of DEAP incremental actuator, (b) Side view, (c) Break system [40].

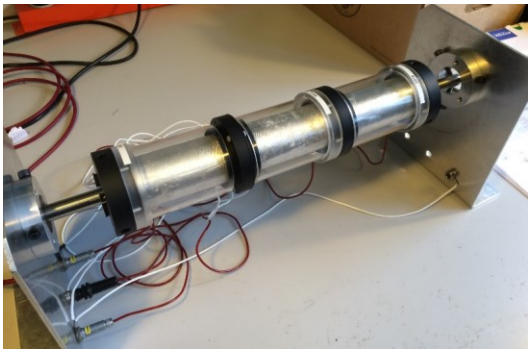

Fig. 19. Setup of the concept 3 DEAP incremental actuator.

auxiliary mechanics and installed on the guiding rod. The rod was fixed on a table in horizontal position. Figure 19 shows the integrated mechanical system with transducers being installed. In order to prevent an electrical breakdown in the actuator, the experiments were performed for lower electrical field i.e. 30 V/μm while the maximum allowable electric field for the used DEAP material is 50 V/μm. After the first set of experiments with the same HV drivers used for concept 1, one of the actuator failed due to an electrical breakdown at 30 V/µm. After an investigation of the actuator, it was observed that the DEAP film had been burned severely in a local spot, and damaged the actuator. The actuator was replaced with the reserved actuator and the experiments were repeated. However, the second actuator got the same defects. Based on the failures in the actuator and the fact that no further actuator prototyping was possible in Danfoss PolyPower due to its shutdown, it was not possible to continue with system tests and as such the test campaign of concept 3 was terminated.

VII. Conclusions

A brief overview of the widely used conventional linear actuator technologies, and their advantages and disadvantages are discussed. An overview of electroactive polymer (EAP) based crawling linear and rotary motors is provided. A new incremental actuator based on DEAP is proposed. The conceptual design of an axial DEAP actuator is discussed. Several characteristics of an axial DEAP actuator are provided and compared with the prototype measurements. The characteristics of different scaled DEAP actuator designs are discussed. The estimated velocities and output forces for all scaled incremental motor designs are provided. The basic operation and control patterns of the proposed DEAP incremental actuator concept are explained. The HV bidirectional DC-DC converters and their design for driving the DEAP incremental motor have been discussed. Energy efficiency measurement results are provided for the non-optimized and optimized HV drivers. The high energy efficiency of the optimized DC-DC converter shows promising advantages for the DEAP incremental motor compared with the conventional actuator technologies.

The proposed DEAP incremental actuator concept has been designed, built and tested. It is demonstrated that the DEAP is feasible for providing incremental motion with variable speed and bidirectional (forward and reverse) motion. The DEAP incremental actuator prototype moved with a maximum velocity of 1.5 mm/s, at 2.87 Hz incremental driving frequency, when all actuators are driven at 1.8 kV. However, it is expected that the maximum speed of the same incremental motor could rise to 3 mm/s when all actuators would be driven at 2.4 kV. Furthermore, the incremental driving frequency is expected to increase 3 to 4 times with improved polymer material within 3 to 5 years. Two new concepts of DEAP incremental actuators are proposed, and their unique features are explained. The concept 2 is proposed for incremental motion inside or outside cylindrical tubes, and the concept 3 is proposed for incremental motion on both straight and curved guides with better compactness. The concepts 2 and 3 incremental actuators are aimed for better performance compared to the concept 1 prototype. The concept 3 has been tested and unfortunately failed. Nevertheless, more research work needs to be conducted, to obtain excellent performance results, in order to compete with the conventional linear and/or EAP actuators. In conclusion, the incremental actuators based on DEAP are promising, and they will have numerous applications when a reliable, and low-cost polymer material can be produced.

Acknowledgement

The authors would like to thank the industrial partner Danfoss PolyPower A/S for providing the actuators and system integration setups. Thanks to the anonymous reviewers for their suggestions in greatly improving the manuscript.

References

[1] JenaTec, Online available: http://www.jena-tec.co.uk/linear-actuators.php [accessed 09 May 2015].

[2] AGI American Grippers, Online available: http://localautomation.com/featured/agi-pneumatic-linear-actuator-agi-american-grippers-inc.html [accessed 09 May 2015].

[3] Stemulate, Online available: http://www.stemulate.org/2012/07/02/solid-learning-robot-linear-actuators/ [accessed 09 May 2015].

[4] PI, Online available: http://www.pi-usa.us/products/PiezoActuators/index.php [accessed 12 May 2015].

[5] PI, Online available: http://piceramic.com/products/piezo-controllers.html [accessed 12 May 2015].

[6] Y. Bar-Cohen, "Electroactive Polymer [EAP] Actuators as Artificial Muscles: Reality, Potential, and Challenges," 2nd ed. Washington, DC: SPIE, 2004.

[7] R. E. Pelrine, R. D. Kornbluh, Q. Pei, J. P. Joseph, "High-speed electrically actuated elastomers with strain greater than 100%," *Science*, vol. 287, pp. 836–839, 2000.

[8] F. Carpi, D. DE Rossi, R. Kornbluh, R. Pelrine, P. Sommer-Larsen, Eds, "Dielectric Elastomer As Electromechanical Transducers," Amsterdam, The Netherlands: Elsevier, 2008.

[9] LEAP Technology, Denmark, Online available: http://leaptechnology.com/ [accessed 13 May 2015].

[10] M. Tryson, H. E. Kiil, M. Benslimane, "Powerful tubular core free dielectric electro-active polymer (DEAP) push actuator," in *Proc. SPIE*, vol. 7287, 2009.

[11] R. Sarban, B. Lassen, M. Willatzen, "Dynamic Electromechanical Modeling of Dielectric Elastomer Actuators With Metallic Electrodes," *IEEE/ASME Trans. Mechatronics,* vol. 17, no. 5, pp. 960-967, Oct. 2012.

[12] L. Huang, P. Thummala, Z. Zhang, M. A. E. Andersen, "Battery powered high output voltage bidirectional flyback converter for cylindrical DEAP actuator," in *Proc. IEEE IPMHVC*, pp. 454-457, 3-7 June 2012.

[13] J. E. Huber, N. A. Fleck, and M. F. Ashby, "The selection of mechanical actuators based on performance indices," in *Proc. R. Soc. Lond. A*, vol. 453, pp. 2185-2205, 8 October 1997.

[14] R. D. Kornbluh, R. Pelrine, Q. Pei, R. Heydt, S. Stanford, S. Oh, J. Eckerle, "Electroelastomers: applications of dielectric elastomer transducers for actuation, generation, and smart structures," in *Proc. SPIE*, vol. 4698, pp. 254-270, 2002.

[15] A. T. Conn, A. D. Hinitt, P. Wang, "Soft segmented inchworm robot with dielectric elastomer muscles," in *Proc. SPIE, Electroactive Polymer Actuators and Devices (EAPAD)*, vol. 9056, pp. 90562L, 2014.

[16] Q. Pei, R. Pelrine, S. Stanford, R. D. Kornbluh, M. S. Rosenthal, K. Meijer, R. J. Full, "Multifunctional electroelastomer rolls and their application for biomimetic walking robots," in *Proc. SPIE*, vol. 4698, 2002.

[17] I. A. Anderson, T. A. Gisby, T. G. McKay, B. M. O'Brien, E. P. Calius, "Multi-functional dielectric elastomer artificial muscles for soft and smart machines," *Journal of Applied Physics*, 112, 041101, 2012.

[18] K. Jung, J. C. Koo, J. -do Nam, Y. K. Lee, H. R. Choi, "Artificial annelid robot driven by soft actuators," *Journal of Bioinspiration and Biomimetics*, vol. 2, pp. S42-S49, 2007.

[19] I. A. Anderson, T. C. H. Tse, T. Inamura, B. M. O'Brien, T. McKay, T. Gisby, "A soft and dexterous motor," *Journal of Applied Physics*, 98, 123704, 2011.

[20] R. Wache, D. N. McCarthy, S. Risse, G. Kofod, "Rotary Motion Achieved by New Torsional Dielectric Elastomer Actuators Design," *IEEE/ASME Trans. Mechatronics*, vol. 99, pp. 1-3, Feb. 2014.

[21] P. Thummala, Z. Zhang, M. A. E. Andersen, S. Rahimullah, "Dielectric electro-active polymer incremental actuator driven by multiple high-voltage bi-directional DC-DC converters," in *Proc. IEEE ECCE USA,* pp. 3837-3844, 15-19 Sept. 2013.

[22] M. Karpelson, G. Y. Wei, R. J. Wood, "Driving high voltage piezoelectric actuators in microrobotic applications," *Sensors and Actuators A*, vol. 176, pp. 78– 89, 2012.

[23] L. Eitzen, C. Graf, J. Maas, "Cascaded bidirectional flyback converter driving DEAP transducers," in *Proc. IEEE IECON*, pp. 1226-1231, 7-10 Nov. 2011.

[24] L. Eitzen, C. Graf, J. Maas, "Bidirectional power electronics for driving dielectric elastomer transducers," in *Proc. SPIE*, vol. 8340, p. 834018 1-12, 2012.

[25] R. W. Erickson, D. Maksimovic, "Fundamentals of Power Electronics," 2nd ed. New York: Springer, 2001.

[26] J. Elmes, C. Jourdan, O. Abdel-Rahman, I. Batarseh, "High-Voltage, High-Power-Density DC-DC Converter for Capacitor Charging Applications," in *Proc. IEEE APEC*, pp. 433-439, 2009.

[27] S. K. Chung, H. B. Shin, "High-voltage power supply for semi-active suspension system with ER-fluid damper," *IEEE Trans. Vehicular Technology*, vol. 53, no. 1, pp. 206- 214, Jan. 2004.

[28] T. Bhattacharya, V. S. Giri, K. Mathew, L. Umanand, "Multiphase Bidirectional Flyback Converter Topology for Hybrid Electric Vehicles," *IEEE Trans. Industrial Electronics*, vol. 56, no. 1, pp. 78-84, Jan. 2009.

[29] G. Chen, Y.-S. Lee, S.Y.R. Hui, D. Xu, Y. Wang, "Actively clamped bidirectional flyback converter," *IEEE Trans. Industrial Electronics*, vol. 47, no. 4, pp. 770-779, Aug. 2000.

[30] F. Zhang, Y. Yan, "Novel Forward–Flyback Hybrid Bidirectional DC-DC Converter," *IEEE Trans. Industrial Electronics,* vol. 56, no. 5, pp. 1578-1584, May 2009.

[31] T. Andersen, M. S. Rødgaard, O. C. Thomsen, M. A. E. Andersen, "Low voltage driven dielectric electro-active polymer actuator with integrated piezoelectric transformer based driver," in *Proc. SPIE EAPAD*, vol. 7976, p. 79762N, 2011.

[32] P. Thummala, Z. Zhang, M. A. E. Andersen, "High Voltage Bi-directional Flyback Converter for Capacitive Actuator," in *Proc. IEEE European Power Electronics conference,* pp. 3-6 Sept. 2013.

[33] L. Huang, Z. Zhang, M. A. E Andersen, "Design and development of autonomous high voltage driving system for DEAP actuator in radiator thermostat," in *Proc. IEEE Applied Power Electronics Conference and Exposition (APEC)*, pp. 1633-1640, 16-20 March 2014.

[34] P. Thummala, H. Schneider, Z. Zhang, Z. Ouyang, A. Knott, M. A. E. Andersen, "Efficiency Optimization by Considering the High Voltage Flyback Transformer Parasitics using an Automatic Winding Layout Technique," *IEEE Trans. Power Electronics*, vol. 30, no. 10, pp. 5755-5768, Oct. 2015.

[35] P. Thummala, H. Schneider, Z. Zhang, and M. A. E. Andersen, "Investigation of Transformer Winding Architectures for High Voltage (2.5 kV) Capacitor Charging and Discharging Applications," *IEEE Trans. Power Electronics*, 2015 (DOI: 10.1109/TPEL.2015.2491638).

[36] N. O. Sokal, R. Redl, "Control algorithms and circuit designs for optimal flyback-charging of an energy storage capacitor (e.g., for flash lamp or defibrillator)," *IEEE Trans. Power Electronics*, vol. 12, no. 5, pp. 885-894, Sep. 1997.

[37] P. Thummala, D. Maksimovic, Z. Zhang, M. A. E. Andersen, "Digital control of a high-voltage (2.5 kV) bidirectional flyback DC-DC converter for driving a capacitive incremental actuator," *IEEE Trans. Power Electronics,* 2016 (DOI: 10.1109/TPEL.2016.2520497).

[38] C. M. Druitt, G. Alici, "Intelligent Control of Electroactive Polymer Actuators Based on Fuzzy and Neurofuzzy Methodologies," *IEEE/ASME Trans. Mechatronics*, vol. 19, no. 6, pp. 1951-1962, Dec. 2014.

[39] J. P. L. Bigue, J. S. Plante, "Experimental Study of Dielectric Elastomer Actuator Energy Conversion Efficiency," *IEEE/ASME Trans. Mechatronics*, vol. 18, no. 1, pp. 169-177, Feb. 2013.

[40] B. Rechenbach, M. Willatzen, R. Sarban, C. Liang, B. Lassen, "Geometry optimization of tubular dielectric elastomer actuators with anisotropic metallic electrodes," in *Proc. SPIE Electroactive Polymer Actuators and Devices (EAPAD)*, vol. 9056, pp. 905606-905606-13, Mar. 2014.

[41] Danfoss PolyPower, Denmark, [Shutdown from Jan. 2015].

[42] Y. H. Iskandarani, R. W. Jones, E. Villumsen, "Modeling and experimental verification of a dielectric polymer energy scavenging cycle", in *Proc. SPIE EAPAD*, vol. 7287, pp. 72871Y-1–72871Y-12, 2009.

[43] M. Tryson, H. -E. Kiil, M. Benslimane, "Powerful tubular core free dielectric electro activate polymer (DEAP) push actuator," in *Proc. SPIE EAPAD*, vol. 7287, pp. 72871F-72871F-11, April, 2009.

[44] P. Thummala, D. Maksimovic, Z. Zhang, M. A. E. Andersen, S. Rahimullah, "Design of a High Voltage Bidirectional DC-DC Converter for Driving Capacitive Incremental Actuators Usable in Electric Vehicles (EVs)," in *Proc. IEEE IEVC*, 14-18 Dec. 2014.

[45] Linear Technology, "LT3751 High Voltage Capacitor Charger with Regulation," Linear Technology Corporation, USA. http://cds.linear.com/docs/en/datasheet/3751fc.pdf [accessed 20 May 2015].

[46] IXYS, IXTV03N400S, 4 kV MOSFET, Online available: http://ixapps.ixys.com/DataSheet/DS100214A-(IXTH_V03N400_S).pdf [accessed 20 May 2015].

[47] IXYS, IXTA02N450HV, 4.5 kV MOSFET, Online available: http://ixapps.ixys.com/DataSheet/DS100498(IXTA-T02N450HV).pdf [accessed 20 May 2015].

[48] H. C. Lo, T. A. Gisby, E. P. Calius, I. A. Anderson, "Transferring electrical energy between two dielectric elastomer actuators", *Sensors and Actuators A: Physical*, Vol. 212, pp. 123-126, 2014.